Stem Cell Research (2014) 13, 111–122

Available online at www.sciencedirect.com

ScienceDirect

www.elsevier.com/locate/scr

The granulocyte macrophage–colony stimulating factor surface modified MB49 bladder cancer stem cells vaccine against metastatic bladder cancer

Yong-tong Zhu [1], Zhen Zhao [1], Xin-yang Fu [1], Yang Luo, Cheng-yong Lei, Wei Chen, Fei Li, Shi-yu Pang, San-san Chen, Wan-long Tan*

Department of Urology, Nanfang Hospital, Southern Medical University, Guangzhou, Guangdong 510515, P.R. China

Received 17 September 2013; received in revised form 23 March 2014; accepted 14 April 2014
Available online 24 April 2014

Abstract The MB49 bladder cancer cell vaccine was effective against bladder cancer in the mice model in previous studies. However, part of the tumors regrew as the vaccine could not eliminate the cancer stem cells (CSCs). MB49 bladder cancer stem cells (MCSCs) were isolated by a combination of the limited dilution method and the serum free culture medium method. MCSCs possessed higher expression of CD133, CD44, OCT4, NANOG, and ABCG2, the ability of differentiation, higher proliferative abilities, lower susceptibility to chemotherapy, greater migration in vitro, and stronger tumorigenic abilities in vivo. Then streptavidin–mouse granulocyte macrophage–colony stimulating factor (SA–mGM–CSF) MCSCs vaccine was prepared. SA–mGM–CSF MCSCs vaccine extended the survival of the mice and inhibited the growth of tumor in protective, therapeutic, memorial and specific immune response experiments. The level of immunoglobulin G and the ratio of dendritic cells and $CD4^+$ and $CD8^+$ T cells were highest in the experimental group when compared to those in other four control groups, as well as for the cytotoxicity assay. We demonstrated that SA–mGM–CSF MCSCs vaccine induces an antitumor immune response to metastatic bladder cancer.

Introduction

Bladder cancer is one of the most common urologic cancers in the United States and the rest of the world (Siegel et al., 2013), and radical cystectomy with pelvic lymphadenectomy is the standard treatment for this kind of cancer. However, more than half of the patients will develop local or metastatic recurrence (Cagiannos and Morash, 2009). In previous studies, we have shown that the MB49 bladder cancer cell vaccine induces a specific antitumor immunity and is efficiently effective against metastatic bladder cancer in a mice model (Shi et al., 2013; Zhang et al., 2011, 2012). However, we also found that over time part of the tumors experienced regression and regrew because the cancer stem cells (CSCs) could not be eliminated by the

* Corresponding author. Fax: +86 20 61641762.
E-mail address: tanwanlong@gmail.com (W. Tan).
[1] Contributed equally to this work.

http://dx.doi.org/10.1016/j.scr.2014.04.006

vaccine. Relapses of solid tumors may be attributed to the inability of traditional chemotherapies and radiotherapies to eradicate CSCs (McDermott and Wicha, 2010). Our former vaccine was unable to induce specific immunities responsible for eliminating CSCs. Therefore, on the basis of our protein-anchor technology, we developed a vaccine that displayed streptavidin–mouse granulocyte macrophage–colony stimulating factor (SA–mGM–CSF) on the surface of biotinylated MB49 bladder cancer stem cells (MCSCs), and evaluated the antitumor effects of this vaccine in the treatment of MCSCs in a metastatic mouse model.

Materials and methods

Establishment of MCSCs

MB49, a mouse bladder cancer cell line, was a gift from Dr. I. C. Summerhayes from the Lahey Clinic in Burlington, Massachusetts (Shi et al., 2013; Zhang et al., 2011, 2012). MB49 cells were cultured in RPMI1640 containing 10% fetal bovine serum (FBS, Thermo Scientific HyClone, Logan, Utah) at 37 °C in a 5% CO_2 humidified incubator.

The optimal serum free culture medium (SFM) consisted of RPMI1640, epidermal growth factor (20 ng/ml), basic fibroblast growth factor (20 ng/ml), leukemia inhibitory factor (20 ng/ml), B-27 serum-free supplement (20 μl/ml), and bovine serum albumin (4 μg/ml).

For the limited dilution method, MB49 cells were digested with accutase-enzyme cell detachment medium (Accutase, eBioscience, San Diego, California) and the number of cells was counted using a counting chamber. Cell suspensions were diluted with SFM in a ten-fold manner until the terminal density of the cells was 5 cells/ml. Finally, 200 μl of cell suspension was plated into 96-well plates with ultra low attachment surface (Corning Life Sciences, Union City, California), and single cells were marked and observed daily. Most cells were unable to proliferate in SFM, only a small percentage of cells generated clone spheres. These single cells extracted from MB49 cells were called passage 1 MCSCs.

Several passage 1 single cells were cultured in SFM, and the supernatant was removed and supplemented with fresh SFM every 5–7 days. By day 30, single cells had grown into large, visible, single-cell spheres. Spheres were digested with Accutase, dispersed mechanically, and cultured in 24-well plates with ultra low attachment surface (Corning Life Sciences) before forming passage 2 cells.

Passage 2 cells were supplemented with fresh SFM every 3–4 days. By day 15, most cells had grown into visible spheres that were collected, centrifuged, digested, dispersed, and cultured in 6-well plates with ultra low attachment surface (Corning Life Sciences) before forming passage 3 cells. Cells were expanded in T25 culture flasks (Corning Life Sciences) through multiple passages using the same protocol.

Characterizations of MCSCs

Expression of MCSCs markers

Flow cytometry (FCM). MB49 cells and MCSCs were harvested respectively. They were dissociated at a density of 1×10^4 cells in 100 μl autoMACS running buffer (Miltenyi Biotec, Bergisch Gladbach, Germany), labeled with PE mouse anti-prominin-1 (Miltenyi Biotec) and FITC mouse antiCD44 (Miltenyi Biotec), incubated at 4 °C for 20 min, and washed twice with phosphate buffered saline (PBS). PE rat IgG1 κ isotype control (eBioscience) and TITC rat IgG2b κ isotype control (eBioscience) were used as negative control. The ratio of $CD44^+CD133^+$ cells was evaluated using a BD FACSAria cell sorter (Becton-Dickinson, San Jose, California).

Quantitative polymerase chain reaction (qPCR). Total RNA was extracted using the Arcturus PicoPure RNA isolation kit (Applied Biosciences, Carlsbad, New Mexico). RNA quality was verified by the Bioanalyzer RNA Pico Chip (Agilent Technologies, Santa Clara, California). Two micrograms of total RNA were reverse transcribed with Superscript III (Invitrogen, Grand Island, New York). cDNA was amplified with SYBR green PCR master mix (Bio-Rad, Hercules, California) on a 7500 real time PCR system (AB Applied Biosystems, Singapore). Cycling conditions were 95 °C for 10 s (denaturation) and 60 °C for 60 s (annealing and extension). Primer sequences are listed in Table 1. Normalization and fold changes were calculated using the $\Delta\Delta C_t$ method, and GAPDH was used as negative control.

Western blotting (WB). Proteins were separated by 10% sodium dodecyl sulfate–polyacrylamide gel and transferred to polyvinylidene difluoride membranes (Millipore, Billerica, Massachusetts) electrophoretically. Filters were blocked with 5% skim milk in PBS and incubated at 4 °C overnight with the primary antibody anti-OCT4 (Abcam, Cambridge, Massachusetts), anti-NANOG (Abcam), anti-ABCG2 (Abcam), or anti-β-actin antibody (Abcam). Filters were then incubated with conjugated anti-mouse secondary antibodies (Abcam). Protein bands were detected by Fluor Chem FC2 (Alpha Innotech, San Leandro, California), and the intensities of protein blots were analyzed by Image Lab software.

Differentiation

MCSCs were collected, dissociated into single cells, and cultured in RPMI1640 supplemented with 10% FBS that induced

Table 1 Primers of selected genes.

Gene name	Primers (forward/reverse)	Amplicon length
CD133	F: 5′-CGGGATCCGAAAAACTGATCTGT-3′ R: 5′-CCGCTCGAGTTACCTAGTTACTCT CTCC-3′	615 bp
CD44	F: 5′-CCCTGCTACCAGAGACCAAGAC-3′ R; 5′-GCAGGTTCCTTGTCTCATCAGC-3′	401 bp
NANOG	F: 5′-CAGCTGTGTGTACTCAATGATAGAT TT-3′ R: 5′-ACACCATTGCTATTCTTCGGCCAG TTG-3′	179 bp
OCT4	F: 5′-TCAGCCAAACGACCATCTGC-3′ R: 5′TTCTCCAGGTTGCCTCTCAC-3′	205 bp
GAPDH	F: 5′-CCATGGAGAAGGCTGGGG-3′ R: 5′-CAAAGTTGTCATCCATGACC-3′	198 bp

cell differentiation. Meanwhile, MCSC spheres were cultured by the same method.

Functional comparison

Cell proliferation assay. Cells were plated in the optimal SFM at a number of 1×10^3 cells per well in a 96-well plate and incubated for 1, 2, 3, 4, 5, or 6 days respectively. Then 10 μl of cell counting kit-8 reagent (CCK-8, Dojindo Molecular Technologies, Kumamoto, Japan) was added at a fixed time of the day. After 4 hours of incubation, the absorbance value was measured at 450 nm using an EnSpire 2300 multilabel reader (PerkinElmer, Singapore).

Soft agar assay. Cells were resuspended at a density of 1×10^4 cells/ml in 0.66% bottom agar (Beyotime, Jiangsu, China) supplemented with 10% FBS, and on the top 1.32% agar was layered supplemented with 20% FBS in 6-well plates respectively. Plates were incubated for three weeks. Finally the colonies with diameters greater than 50 μm were counted.

Migration abilities in vitro. Cells (1×10^4 cells/well) were seeded in pure RPMI1640 (0.25 ml) in the upper well of a 6.5-mm pore-size polycarbonate membrane chamber inserted in a transwell apparatus (Costar, Cambridge, Massachusetts). RPMI1640 medium containing 10% FBS (0.75 ml) was added in the lower well. Cells were incubated for 24 hours and cells that had migrated to the bottom surface of the insert were fixed in paraformaldehyde for 20 min, stained in Giemsa for 15 min, rinsed in PBS, and inspected via inverted microscopy.

Resistance to chemotherapy abilities. Cells were seeded at a number of 1×10^4 per well in a 96-well plate. After 24 hours, mitomycin (Sigma, Saint Louis, Missouri), cisplatin (Sigma), paclitaxel (Sigma), or doxorubicin (Sigma) was added with different concentrations (Table 2) respectively, and cells were treated for a subsequent 96 hours. Then CCK-8 reagent was added to each well, and after 4 hours of incubation, the absorbance values were measured. Cell viability was expressed as the percentage of absorbance values of the treated wells related to the absorbance of the untreated control wells.

Tumorigenic abilities in vivo. All experimental procedures with animals have been given prior approval by the Ethics Committee of the Southern Medical University under Contract 2011016. Four-week-old nude mice (Center of Experimental Animals, Southern Medical University, Guangzhou, China) were maintained and treated under specific, pathogen-free conditions. Cells were injected subcutaneously into nude mice at a number of 1×10^4 cells in MCSCs and 1×10^6 cells in MB49 cells, respectively. Each group had 5 mice. Tumor xenograft formation was observed every week. At the end of 8 weeks, mice were sacrificed by cervical dislocation. Tumor engrafts were removed, and the volume of the tumors was measured using the formula $d^2 \times D/2$, where d and D were the smallest and the largest diameters respectively (Zhang et al., 2012).

Table 2 Concentrations of chemotherapeutic agents.

Agents	Concentrations			
Paclitaxel	10 nM	100 nM	1 μM	10 μM
Doxorubicin	10 nM	100 nM	1 μM	10 μM
Cisplatin	5 μM	10 μM	15 μM	20 μM
Mitomycin	10 μM	80 μM	640 μM	5.12 mM

Preparation of SA–mGM–CSF MCSCs vaccine

Vaccine preparation

MCSCs were fixed in 30% ethanol for 30 min at room temperature. Ethanol-fixed MCSCs were incubated at a number of 1×10^6 cells with 1 mM fresh EZ-Link Sulfo-NHS-LC-Biotin (Pierce Biotechnology, Rockford, Illinois) for 1 hour at room temperature, and washed 3 times with PBS. The biotinylated cells were incubated with SA–mGM–CSF fusion protein which was prepared in our lab (Hu et al., 2010), and washed 3 times with PBS. Therefore, the product was called SA–mGM–CSF MCSCs vaccine.

Evaluation of SA–mGM–CSF on the surface of MCSCs

The SA–mGM–CSF MCSCs vaccine was washed with PBS and labeled with FITC anti-mGM–CSF monoclonal antibody (BD Biosciences Pharmingen, San Diego, California) for 30 min at room temperature. The biotinylated cells were used as a control group. The presence of SA–mGM–CSF on the surface of MCSCs was evaluated using a BD FACSAria cell sorter.

Bioactive assay of SA–mGM–CSF immobilized on the surface of MCSCs

The vaccine was lysed by three freeze thaw cycles. The membrane fractions were harvested by centrifugation at 15,000 *g* at 4 °C for 5 min and resuspended in complete medium. The SA–mGM–CSF bioactivity was assessed by proliferation of bone marrow cells (BMCs), and SA–green fluorescent protein (GFP) was used as a control group. The membrane fractions were added to BMCs in a 96-well plate, and incubated at 37 °C in a 5% CO_2 humidified incubator for 3 days. Cell viability was measured by the CCK-8 assay.

Level of GM–CSF on SA–mGM–CSF MCSCs vaccine

The level of GM–CSF antibody on the vaccine was measured by WB as described previously. The primary antibodies were anti-GM–CSF (Abcam) and anti-beta II tubulin (Abcam), and SA–GFP was used as a control group.

Animal experiment

Subcutaneous and lung metastatic mouse model of MCSCs

C57BL/6 female mice were injected with 1×10^5 MCSCs into the hind leg to make a subcutaneous model. Mice were injected intravenously in the tail vein with 2×10^4 MCSCs to make a pulmonary model.

Protective immune response experiment

All mice from the pulmonary and subcutaneous model were divided into five groups and each group had 15 mice,

respectively. The treated group was given SA–mGM–CSF MCSCs vaccine. The other four control groups were received SA–mGM–CSF MB49 cells vaccine, ethanol-fixed MCSCs, SA–mGM–CSF or PBS.

Healthy mice were injected subcutaneously with 1×10^5 SA–mGM–CSF MCSCs vaccines on days 0, 4 and 8, followed by injection with MCSCs on day 12 to prepare a subcutaneous or pulmonary model as described previously. The volume of subcutaneous tumors was measured like before. The survival state was observed daily, and the survival time was recorded until day 60.

Immunotherapy experiment

All mice in the pulmonary and subcutaneous model were divided into five groups and each group had 15 mice as described above. Subcutaneous and lung metastatic model mice were established respectively as described previously. They were injected subcutaneously with 1×10^5 SA–mGM–CSF MCSCs vaccines on days 0, 4, 8 and 12. The volume of subcutaneous tumors and the survival state was observed the same as before.

Tumor-specific lymphocyte cytotoxicity assay. On day 19 of the immunotherapy experiment, splenocytes were isolated and stimulated by the inactivated MCSCs plus hIL-2 (R&D systems, Minneapolis, Minnesota) for 5 days. Splenocytes served as effector cells, and MCSCs served as target cells. Both cells were seeded in a 96-well plate at the desired effector/target cells ratio. After 4 hours of incubation, the supernatant was collected. Then the lactate dehydrogenase activity was measured by cytotox 96 non-radioactive cytotoxicity assay (Promega, Madison, Wisconsin). The percentage of tumor-specific cytotoxic T lymphocytes (CTL) was calculated as follows: percentage of CTL = (experimental −effector spontaneous − target spontaneous) / (target maximum − target spontaneous) × 100%.

Enzyme-linked immunosorbent assay (ELISA) for serum Immunoglobulin G (IgG) antibodies. On day 19 of the immunotherapy experiment, 100 μl blood was collected and congealed for 20 min at room temperature. Then the supernatant was harvested by centrifugation at 3000 rpm for 5 min. The concentrations of IgG were examined with an ELISA kit (Abcam) according to the manufacturer's protocol. The optical density (OD) value was measured at 450 nm with a microplate reader.

FCM of dendritic cells (DCs). On day 19 of the immunotherapy experiment, splenocytes were isolated, and red blood cells were lysed by FCM lysing solution (Santa Cruz, Dallas, Texas). Splenocytes were labeled with FITC anti-mCD80 (Biolegend, San Diego, California) and PE anti-mCD11c (Biolegend) using the manufacturer's instruction. The ratio of $CD11c^+CD80^+$ cells was evaluated using a BD FACSAria cell sorter.

FCM of T cell subsets. On day 19 of the immunotherapy experiment, blood was collected and stained simultaneously with PE anti-mCD4 (eBioscience) and FITC anti-mCD8 (eBioscience). Then red blood cells were lysed by FCM lysing solution and centrifuged. The ratio of $CD4^+$ and $CD8^+$ cells was evaluated using a BD FACSAria cell sorter.

Immunohistochemistry. Sections (4 μm thick) were cut onto polylysine-coated microscope slides. After deparaffinization in xylene and hydration through graded alcohol, sections were washed and then exposed with ready-to-use proteinase K solution to enhance antigenicity. Endogenous peroxidase was inactivated by 3% hydrogen peroxide for 5 min and non-specific binding was blocked with 5% normal goat serum in PBS for 15 min. Then sections were incubated at 37 °C for 1 hour with anti-GM–CSF (Abcam) at a 1:100 dilution. After washing with PBS, sections were incubated with anti-mouse secondary antibody (Abcam), followed by incubation with HRP conjugated streptavidin. Finally, sections were colored using DAB, washed in running tap water and counterstained with hematoxylin and mounted.

Memory immune response experiment

On day 60 after tumor challenge, the tumor-free mice from the subcutaneous group or the survived mice from the lung metastatic group were injected intravenously in the tail vein with 1×10^5 MCSCs again. The untreated mice were used as a negative control, and each group had 10 mice. The survival time was recorded.

Specific immune response experiment

On day 60 of the immunotherapy experiment, 5 tumor-free mice or the survived mice were injected subcutaneously with MCSCs in the right hind leg and RM-1 cells in the left hind leg. The volume of subcutaneous tumors was measured.

Statistical analysis

SPSS19.0 software was used for statistical evaluation. All numeric data was expressed as the mean value ± standard deviation. The statistical analysis was performed by one-way ANOVA (when more than 3 groups) or Students *t*-test (between 2 groups). The survival rates were analyzed using the Kaplan–Meier method, and the log-rank test was used to compare the difference in survival rate between groups. Differences between the values were considered statistically significant when $P < 0.05$.

Results

Establishment of MCSCs in SFM

The limited dilution method showed that only 2–3% of MB49 cells generated CSC spheres in SFM. A passage 1 single MB49 cell formed a CSC sphere within 30 days in SFM (Fig. 1A). MCSCs from several single cells were passaged after 15 days to form new tumor spheres, and most MCSCs generated secondary spheres. (Fig. 1B)

Characterizations of MCSCs

Expression of CSCs markers

As demonstrated by FCM analysis, the fraction of $CD44^+$ cells in MB49 cells was higher than in MCSCs, and MCSCs events

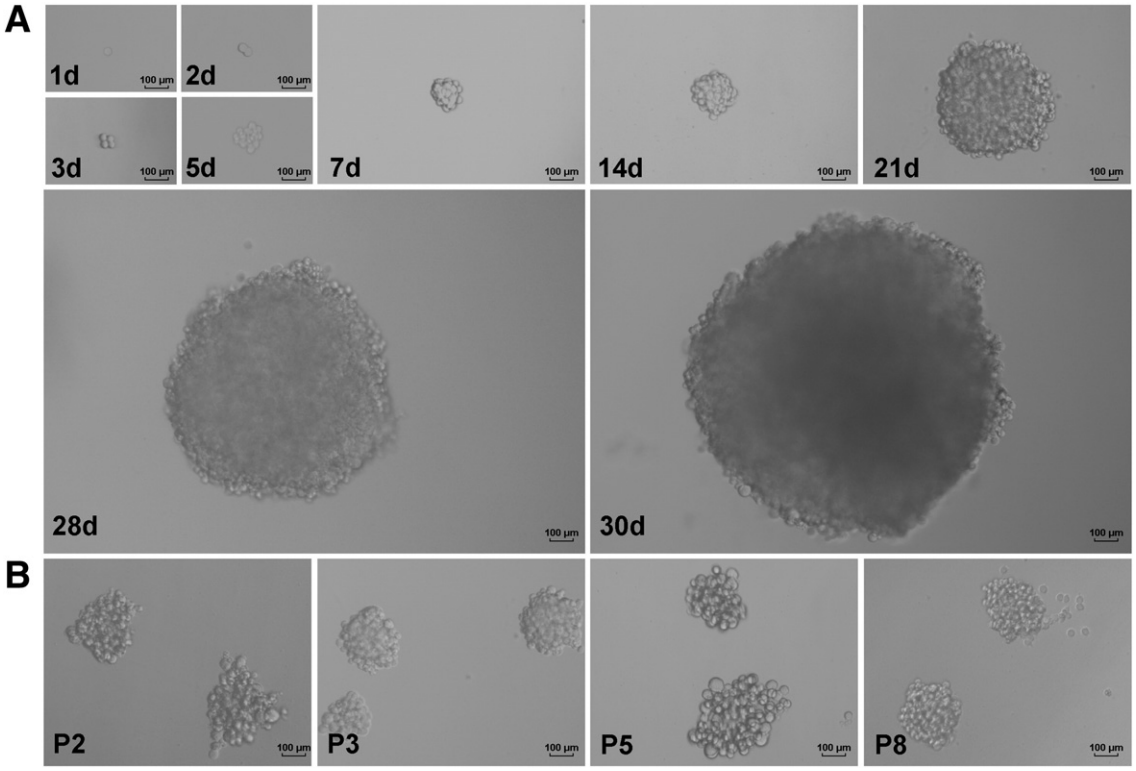

Figure 1 The morphology of MCSCs. (A) A representative image of a cancer stem cell sphere formation originating from a single MB49 cell in SFM. (B) MCSCs generated secondary passages (d = day; P = passage).

collected were smaller on account of the difficulty in proliferation. However, the fraction of $CD133^{+}CD44^{+}$ cells was 19.83 ± 0.68% in MCSCs and 3.57 ± 0.38% in MB49 cells, which was elevated in MCSCs relative to MB49 cells (Fig. 2A).

The relative levels of CD133, OCT4 and NANOG mRNA were respectively 5.2, 4.6 and 4.0 times higher in MCSCs when compared with MB49 cells. However, the level of CD44 was higher in MB49 cells (Fig. 2B).

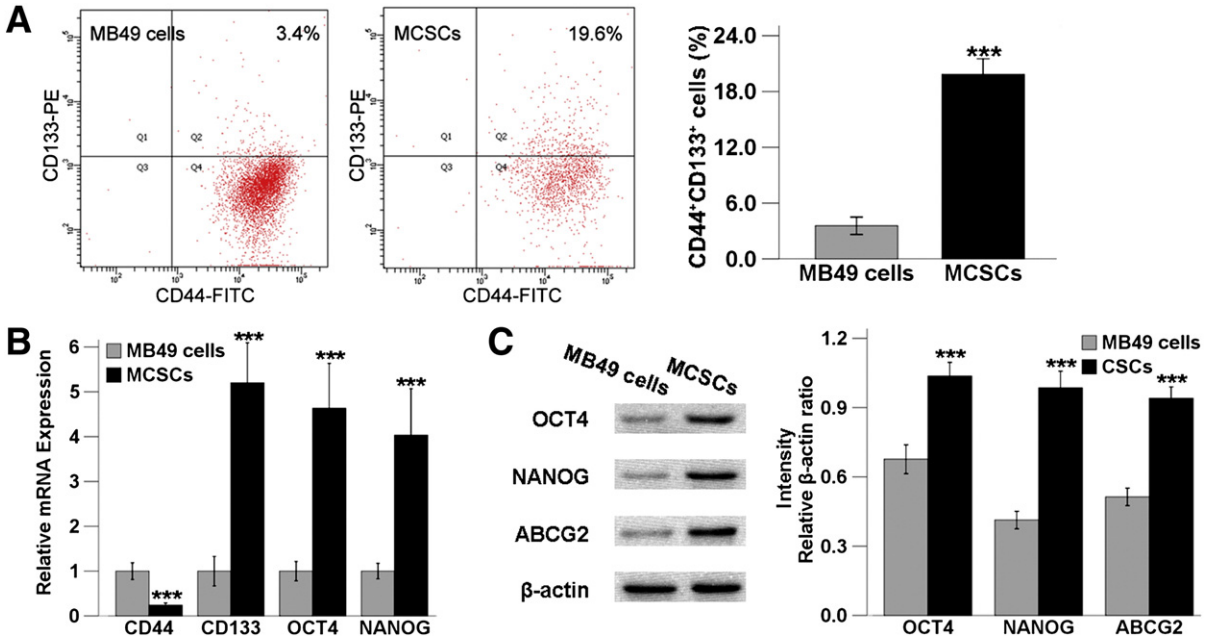

Figure 2 Comparison of specific markers between MCSCs and MB49 cells using (A) FCM, (B) qPCR and (C) WB. (A) (left panel) The representative image of $CD44^{+}CD133^{+}$ cells in FCM analysis. (right panel) The fraction of $CD44^{+}CD133^{+}$ cells in MCSCs was more elevated than those in MB49 cells in FCM analysis. (B) In qPCR analysis, the expression of CD133, OCT4 and NANOG was higher in MCSCs, and CD44 expression was higher in MB49 cells. (C) (left panel) The pattern of OCT4, NANOG and ABCG2 expression in WB analysis. β-Actin was used as a positive control. (right panel) In WB analysis, OCT4, NANOG and ABCG2 were abundantly expressed in MCSCs. $^{***}P < 0.001$ (vs. MB49 cells).

OCT4, NANOG and ABCG2 were all expressed in MCSCs and MB49 cells as demonstrated by WB assay. They were sparsely distributed in MB49 cells, but they were abundantly expressed in MCSCs (Fig. 2C).

Differentiation

MCSCs were globular and floating in SFM. When MCSCs were reseeded in medium containing 10% FBS, they became flat after being differentiated and attached to the culture dish. This morphology resembled the morphology of MB49 cells. The morphology of MCSCs was reverse differentiation to that of MB49 bladder cancer cells (Fig. 3).

Functional comparison

CCK-8 assay showed that MCSCs displayed an increased proliferation rate when compared with MB49 cells in SFM on day 4, 5, 6 (Fig. 4A). The soft agar assay revealed that MCSCs formed bigger and more numerous colonies than MB49 cells did (Fig. 4B). Compared with MB49 cells, both assays showed that MCSCs possessed highly proliferative abilities, either they did not differentiate in the optimal SFM or differentiated to MB49 cells in the medium containing FBS.

More invaded MCSCs were observed when compared to MB49 cells under the same incubation conditions (Fig. 4C). The transwell migration assay displayed that MCSCs contained higher transmembrane activity than MB49 cells.

Compared to MB49 cells, MCSCs showed higher cell viabilities after being treated with different concentrations of mitomycin, cisplatin, paclitaxel or doxorubicin (Fig. 4D). MCSCs demonstrated lower susceptibility to all four traditional anticancer agents.

MCSCs caused a more remarkable tumor volume than MB49 cells did despite the same number of injections (Fig. 4E). Compared with MB49 cells, the histological appearance by hematoxylin and eosin staining displayed greater cell density and deeper nuclear staining in xenograft tumor sections formed by MCSCs (Fig. 4F). Xenograft formation showed that MCSCs possessed strong tumorigenic ability in vivo.

Preparation of SA–mGM–CSF MCSCs vaccine

As demonstrated by FCM analysis, the percentage of MCSCs anchored with SA–mGM–CSF was 89.5 ± 1.5% (Fig. 5A). The membrane bound mGM–CSF stimulated the proliferation of BMCs in a dosage dependent manner which was demonstrated by using the CCK-8 assay (Fig. 5B). The level of GM–CSF antibody on the vaccine was abundantly expressed as displayed by WB assay (Fig. 5C). These results demonstrated that SA–mGM–CSF could be efficiently anchored on the surface of MCSCs and retain its bioactivity.

Animal experiment

Protective immune response with SA–mGM–CSF MCSCs vaccines

Pulmonary model mice in the treated group had a significantly longer survival rate (median of 49 days) when compared to the mice in the four control groups. The

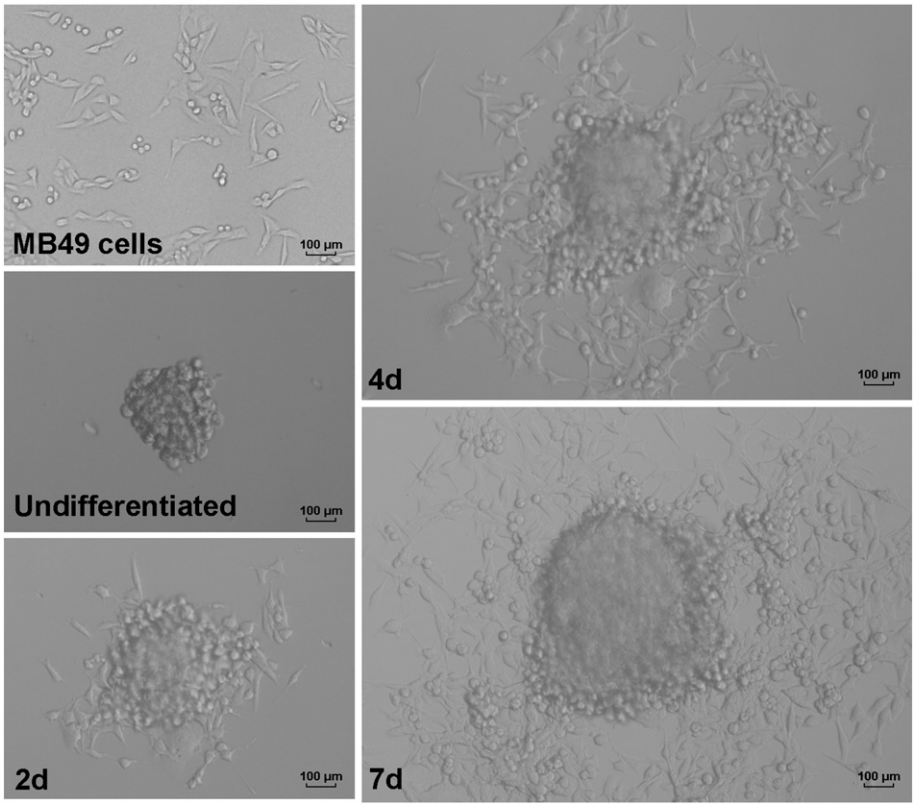

Figure 3 The morphology of MCSCs was reverse differentiation to that of MB49 cells when cultured in medium containing 10% FBS (d = day).

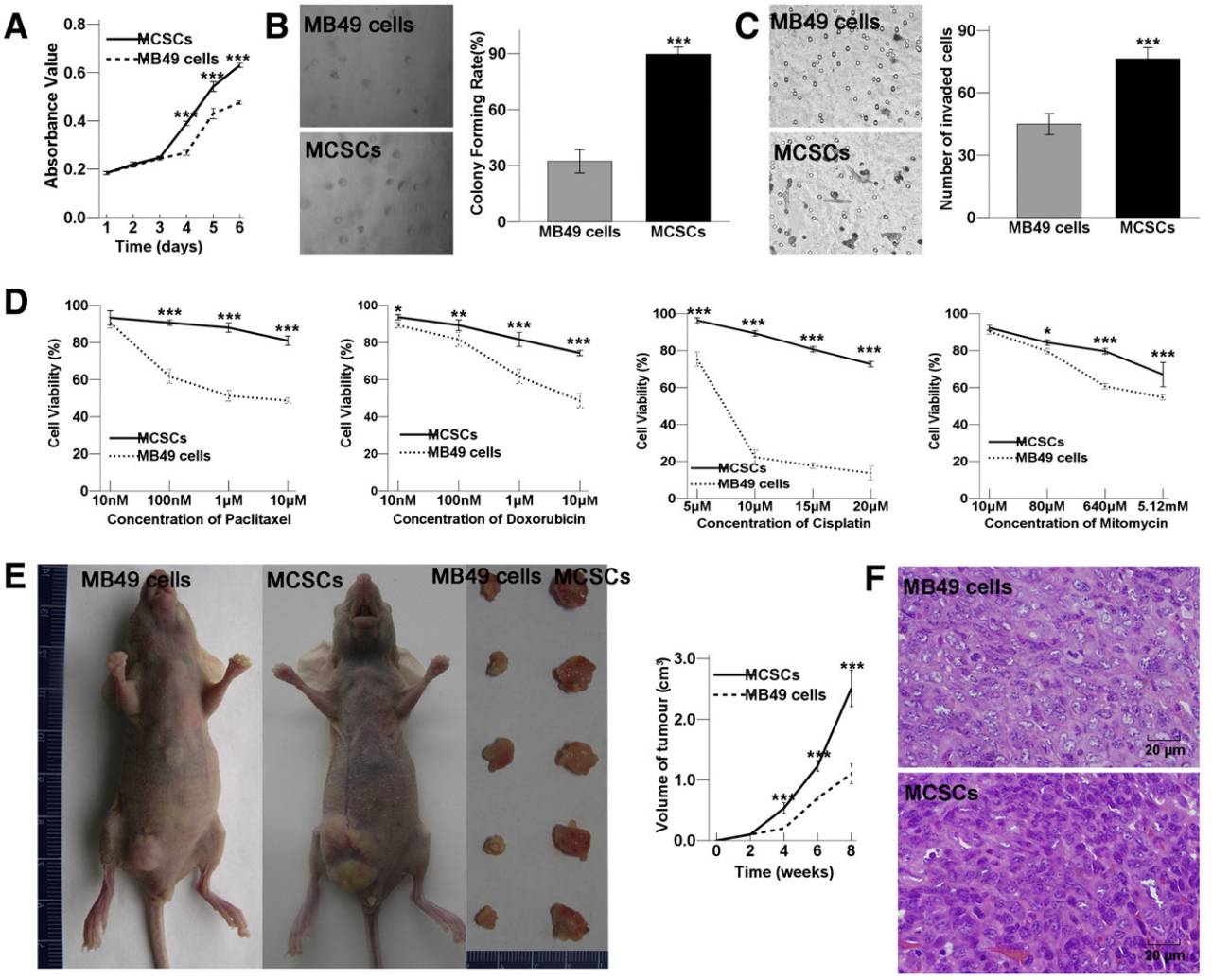

Figure 4 Functional comparisons between MCSCs and MB49 cells in (A and B) proliferative abilities, (C) migrational abilities, (D) anti-cancer chemotherapy abilities, and (E and F) tumorigenic abilities. (A) MCSCs contain higher absorbance value at days 4, 5, and 6 in cell proliferation assay. (B) (left panel) The light images of soft agar assay. (right panel) MCSCs formed more numerous colonies than MB49 cells. (C) (left panel) The light images of transwell migration assay. (right panel) The numbers of invaded MCSCs were higher than MB49 cells. (D) Compared to MB49 cells, MCSCs showed higher cell viabilities after treatment with various concentrations of anti-cancer drugs including paclitaxel, doxorubicin, cisplatin and mitomycin. (E) (left panel) The light images of subcutaneously tumorigenicity by xenograft formation in nude mice. (right panel) MCSCs caused remarkable bigger tumor volume than MB49 cells. (F) Microphotographs of H&E stained tumor tissue sections displayed greater cell density and deeper nuclear staining in xenograft tumor sections formed by MCSCs. $^{*}P < 0.05$, $^{**}P < 0.01$, $^{***}P < 0.001$ (vs. MB49 cells).

median survival of mice in SA–mGM–CSF MB49 cells vaccine, ethanol-fixed MCSCs, SA–mGM–CSF or PBS groups were 42, 34, 35 or 30 days, respectively (Fig. 6A).

The tumors from the subcutaneous model mice in the treated group reached a maximum mean volume of 181 mm^3, and had a significantly smaller tumor volume trend when compared to the four control groups. The maximum mean volume of the four control groups was 430, 662, 705 and 931 mm^3, respectively (Fig. 6B).

Immunotherapy with SA–mGM–CSF MCSCs vaccines

The survival of mice from the pulmonary model in the treated group was significantly longer when compared to those in the four control groups. This also applied for the tumor size in the subcutaneous model (Fig. 6CD). Similar with previous protective immune response, the treated group had the longest survival and the smallest tumor volume.

Tumor-specific lymphocyte cytotoxicity assays. The percentage of CTL in the treated group was significantly higher when compared to the four control groups (Fig. 7A). These results demonstrated that SA–mGM–CSF vaccine could establish a stronger tumor-specific T-cell immunity.

Detection of serum IgG antibodies. The level of specific IgG antibodies in the serum of the treated group was more obvious than in the serum of the four control groups

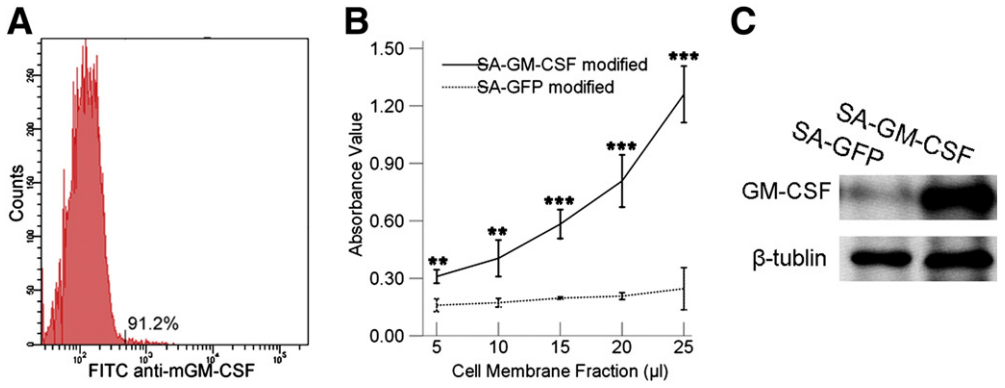

Figure 5 Analysis of SA–mGM–CSF MCSCs vaccine by (A) FCM, (B) CCK-8 and (C) WB assays. (A) The representative image of MCSCs anchored with SA–mGM–CSF. (B) SA–mGM–CSF MCSCs vaccine contained higher absorbance value in proliferative activity, while SA–GFP was the control group. (C) The pattern of GM–CSF expression in WB analysis. β-Tublin was used as a positive control. $^{**}P < 0.01$, $^{***}P < 0.001$ (vs. SA–GFP group).

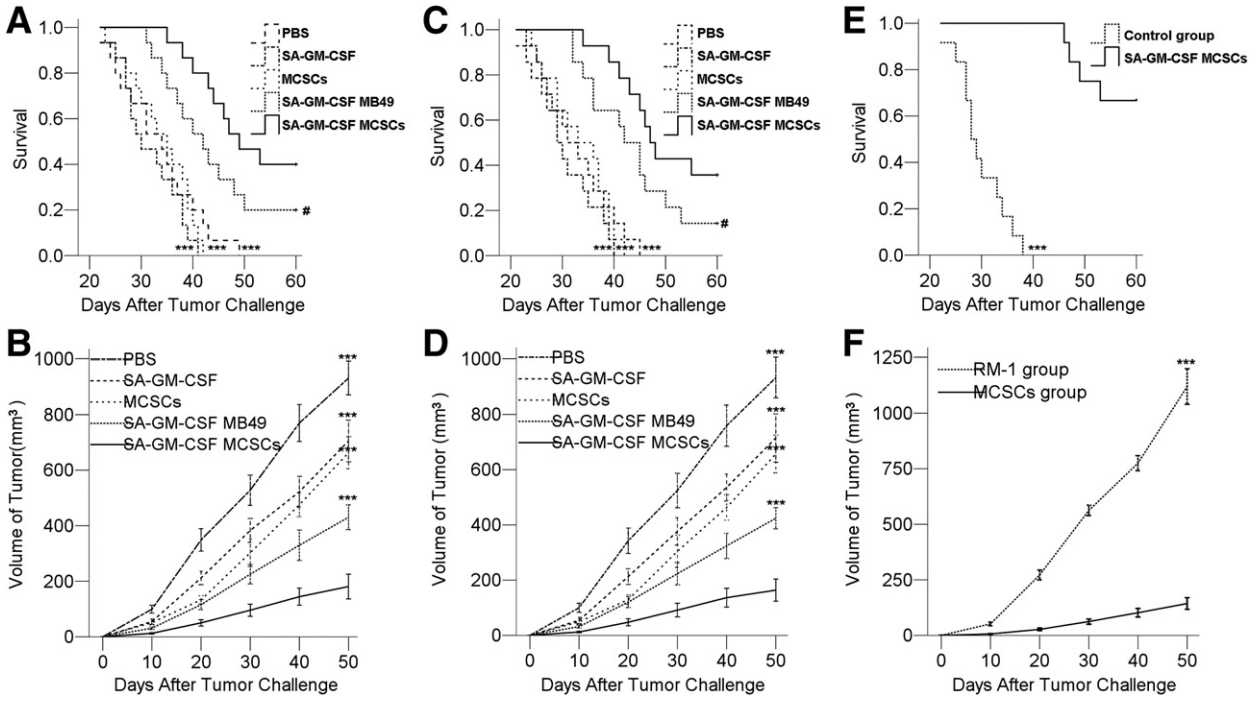

Figure 6 The antitumor potency of SA–mGM–CSF MCSCs vaccine in (A and B) protective, (C and D) therapeutic, (E) memorial and (F) specific immune response experiment. (A, C, and E) Pulmonary model mice in treated group had a significantly longer survival compared to the control groups. (B, D, and F) Subcutaneous model mice in treated group had a significantly smaller tumor volumes trend compared to the control groups. $^{\#}P > 0.05$; $^{***}P < 0.001$ (vs. treated group).

Figure 7 The antitumor potency of SA–mGM–CSF MCSCs vaccine using (A) cytotoxicity assay, (B) ELISA and (C and D) FCM. (A) Both in pulmonary model mice (left panel) and subcutaneous model mice (right panel), the percentage of CTL in treated group was significantly higher compared to the control groups. (B) The level of specific IgG antibodies in sera in the treated group was increased when compared to the four control groups in pulmonary model mice (left panel) and subcutaneous model mice (right panel). (C) Analysis by FCM, (left panel) the representative image of DCs ($CD11c^+CD80^+$ cells) in pulmonary model mice (up panel) and subcutaneous model mice (down panel). In both model mice, (right panel) the number of DCs in the treated group was more elevated than those in the control groups. (D) Analysis by FCM, (left panel) the representative image of $CD4^+$ and $CD8^+$ T cells in pulmonary model mice (up panel) and subcutaneous model mice (down panel). In both model mice, (right panel) the number of $CD4^+$ and $CD8^+$ T cells in the treated group was more elevated than those in the control groups. $^{***}P < 0.001$ (vs. treated group).

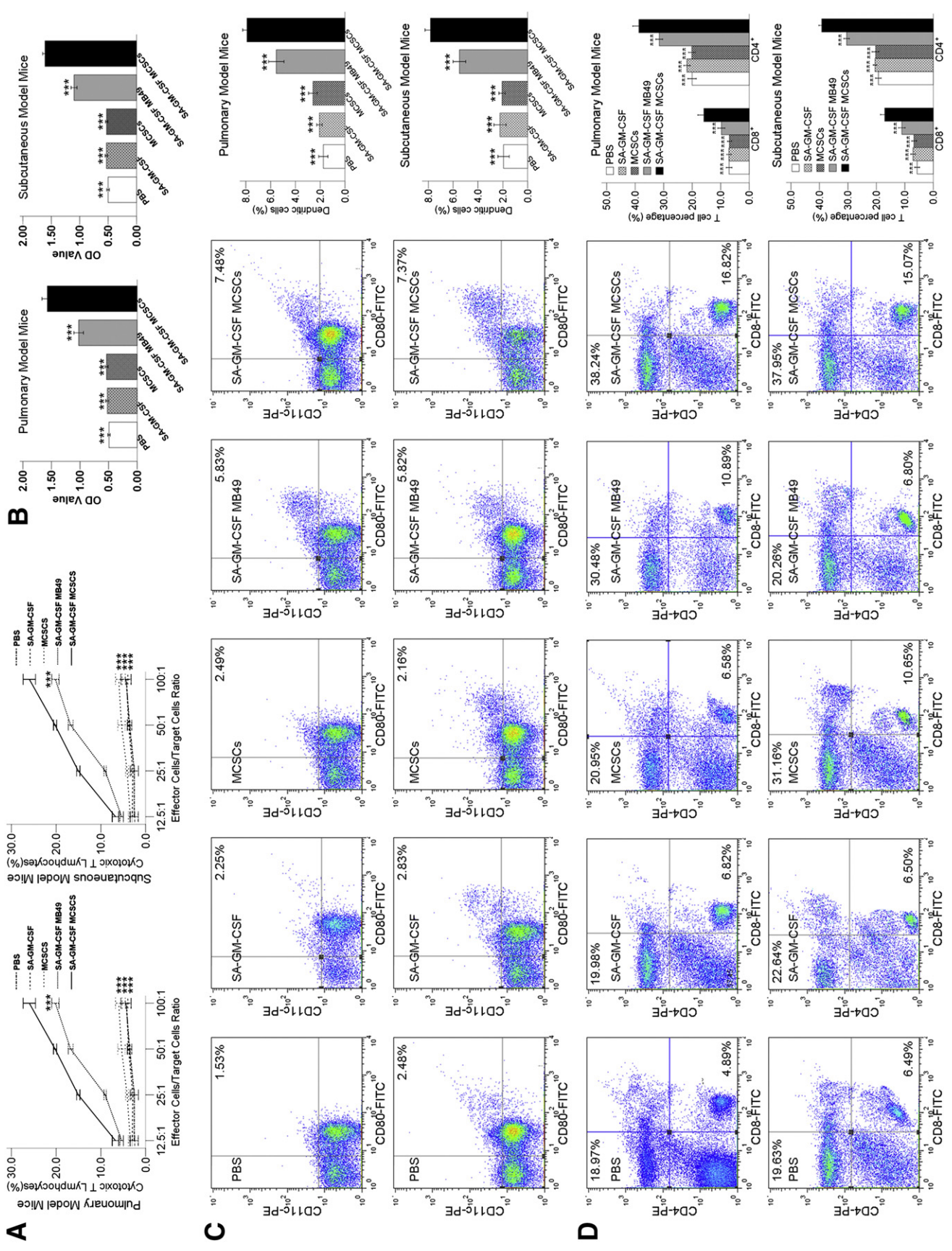
A
Pulmonary Model Mice
Subcutaneous Model Mice
Cytotoxic T Lymphocytes(%)
Effector Cells/Target Cells Ratio
12.5:1
25:1
50:1
100:1
PBS
SA-GM-CSF
MCSCs
SA-GM-CSF MB49
SA-GM-CSF MCSCs
B
Pulmonary Model Mice
Subcutaneous Model Mice
OD Value
C
D
Dendritic cells (%)
T cell percentage (%)
CD8+
CD4+
CD11c-PE
CD80-FITC
CD4-PE
CD8-FITC
1.53%
2.48%
2.25%
2.83%
2.49%
2.16%
5.83%
5.82%
7.48%
7.37%
18.97%
19.63%
19.98%
22.64%
20.95%
31.16%
30.48%
20.26%
38.24%
37.95%
4.89%
6.49%
6.82%
6.50%
6.58%
10.65%
10.89%
6.80%
16.82%
15.07%

(Fig. 7B). The increase of IgG could strengthen the antitumor immunity effect in mice.

Number of DCs. As shown by FCM analysis, the number of mature DCs ($CD11c^+CD80^+$) was significantly more in the treated group than in the four control groups (Fig. 7C). Results demonstrated that SA–mGM–CSF MCSCs vaccine could increase the mature DCs population.

Number of T cell subsets. As demonstrated by FCM analysis, the proportion of $CD4^+$ and $CD8^+$ T cells in the treated group was increased when compared with the four control groups (Fig. 7D). The increase of $CD4^+$ and $CD8^+$ T lymphocytes could enhance the antitumor immunity effect in mice.

Expression of GM–CSF in subcutaneous tumor. As testified by immunohistochemistry, the expression of GM–CSF could be found in sections from subcutaneous tumors from the treated group, and showed significant differences when compared with sections from the four control groups (Fig. 8).

Memory immune response with SA–mGM–CSF MCSCs vaccines

The survival time of mice in the experimental group was significantly longer than in the control group after a second challenge of MCSCs (Fig. 6E). This result demonstrated that SA–mGM–CSF MCSCs vaccine could produce long term memory immunity to MCSCs.

Specific immune response with SA–mGM–CSF MCSCs vaccines

The volume of the tumors at MCSCs injecting side in the right leg was obviously smaller than that at the RM-1 cell injecting side in the left leg (Fig. 6F). This result demonstrated that SA–mGM–CSF MCSCs vaccine could establish a strong tumor specific T cell immunity.

Discussion

The present study examined the feasibility and efficacy of an active vaccine immunotherapy targeting CSCs. To our knowledge, this is the first report of a therapy targeting a characterized population of CSCs in bladder cancer (Vik-Mo et al., 2013).

The limited dilution method showed that only a small percentage of MB49 cells generated CSC spheres, and this proportion was similar to other published results (She et al., 2008). The origin of MCSCs in this study was derived from several single cells. To facilitate the transition of MCSCs to cells suitable for vaccine applications, advances in expanding MCSCs have become an absolute necessity. There are three methods that have been used to isolate CSCs from tumors: specific cell surface markers, SFM, and side population cells (Li et al., 2012). Considering that serum caused irreversible differentiation of stem cells, SFM selection might be useful for CSCs expansion and would allow for the maintenance of an undifferentiated stem cell status (Yanamoto et al., 2011).

CD133 and CD44 have been used to identify CSCs from other cancer tissues (Brescia et al., 2012; Han et al., 2011). However, CD44 cannot be regarded as a universal bladder cancer stem cell marker (Hatina and Schulz, 2012), and the fraction of $CD44^+$ cells in MCSCs was lower as well. Interestingly, our results showed an elevated $CD44^+CD133^+$ expression in MCSCs. Targeting $CD133^+$ and $CD44^+$ cancer cells or the pathways sustaining $CD44^+CD133^+$ subpopulation might be an efficient strategy for colorectal cancer therapy (Ou et al., 2013). $CD44^+CD133^+$ both positive cells might be a CSC-enriched populations in MB49 bladder cancer cells. Only cells expressing $CD44^+CD133^+$ would be counted as MCSCs by FCM. OCT4 plays a significant role in self-renewal (Felthaus et al., 2011), and NANOG is identified as a key molecule to maintain self-renewal and to block differentiation (Gong et al., 2012). These genes can potentially lead to tumorigenesis and affect some cancer behaviors, such as resistance to therapies or cancer recurrence (Li et al., 2012). They were upregulated not only at the protein level (WB) but also at the mRNA transcript level (qPCR) in MCSCs.

The capability to differentiate is another important feature of CSCs (Bentivegna et al., 2010). MCSCs in different culture conditions showed changed differentiation features. Furthermore, we applied techniques to functionally characterize the MCSCs populations (Dalerba et al., 2007; Visvader and Lindeman, 2008). MCSCs had typical CSCs' characterizations that were capable of self-regeneration with a higher proliferative capacity and a greater colony forming potential. MCSCs showed greater capacity to penetrate wells, which indicated that these cells were the most likely to migrate.

Chemotherapy kills the majority of cells in a tumor, but it does not kill CSCs, which might be the mechanism behind the resistance to chemotherapy (Sung et al., 2008; Okamoto et al., 2009). MCSCs had a lower susceptibility to mitomycin, cisplatin, paclitaxel, and doxorubicin. ATP-binding cassette (ABC) transporters explained the mechanism that many chemical drugs were pumped out of cells by ABC transporters (Scopelliti et al., 2009). MCSCs showed a higher level of ABCG2 expression at the protein level (WB), and the upregulation of ABCG2 was associated with the resistance of MCSCs to anti-cancer drugs. The standard experimental method for the isolation of CSCs was used to test the tumorigenicity of cancer cells in immunodeficient mice (Lobo et al., 2007). MCSCs showed the greatest ability to form tumors in subcutaneous tissues of nude mice. Taken

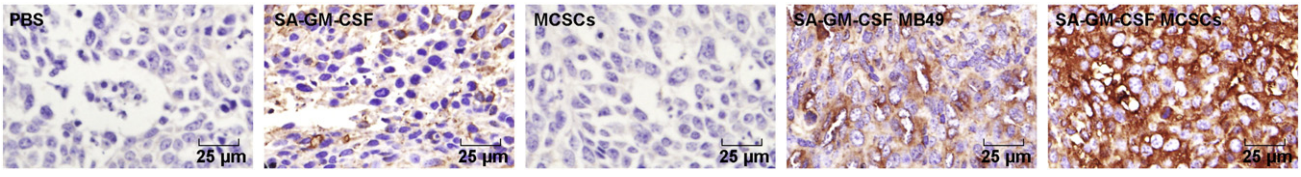

Figure 8 The expression of GM–CSF in histological sections by immunohistochemistry analysis.

together, these data showed that cultured MCSCs displayed specific CSC properties.

Although SA–mGM–CSF MB49 cells vaccine in earlier studies induced a specific antitumor immunity to MB49 cells and obliterated the tumor, vaccine could not induce specific immunity responsible for MCSCs. Therefore, some mice still got tumors after a period of time. In order to kill MCSCs, SA–mGM–CSF MCSCs vaccine was developed on the basis of original vaccine.

Compared with the original vaccine, the SA–mGM–CSF MCSCs vaccine efficiently prolonged the survival of the mice and inhibited the tumor growth. Furthermore, the mice cured by vaccine could resist a second attack of MCSCs but not RM-1 cells, and effector cells also inhibited MCSCs growth which was showed by using a cytotoxicity assay in vitro. The level of IgG in the serum reflected the level of total Ig as it accounted for more than 80% of total Ig. This study showed that the level of IgG increased significantly in the treated group when compared with the control groups. These results indicated that the vaccine immunotherapy could induce tumor specific immunity against MCSCs.

GM–CSF could motivate mature DCs from immature cells (Fleetwood et al., 2005), and plays a decisive role in the development of DCs in the immune response. However, the impact of anticancer immunity rests with the action of T lymphocytes. DCs are intermediates of T lymphocytes immunity and the most effective antigen presenting cells (Hong et al., 2012). The vaccine brought about a T lymphocyte mediated immune response, such as the increase in $CD4^+$ and $CD8^+$ T cells and the reaction of effector T cells aiming at CSCs (Weng et al., 2013). The vaccine based on $CD4^+$ T cell would stimulate standing functional CTL memory via CD40L (Xie et al., 2013). So $CD4^+$ and $CD8^+$ T lymphocytes cells are the main effector cells in antitumor immunity. The vaccine filled with CSCs antigens could lead to a robust antitumor T cell immunity (Pellegatta et al., 2006). Therefore, mGM–CSF, DCs and T lymphocytes have a close relationship with the antitumor response. MCSCs can be identified and killed by $CD4^+$ and $CD8^+$ T lymphocytes, and immunosuppressive effects of MCSCs can be overcome in mice tumor models.

Conclusion

In this study, a therapeutic MCSCs vaccine was successfully generated and used to obliterate MCSCs to prevent tumor regrowth. However, the exact mechanism is still unknown. More clarity of the functional manner could promote its clinical use. A vaccine made up of patient specific antigens or general cancer antigens may be the direction for the development of a clinical available vaccine in the future.

Acknowledgments

This study was supported by the National Natural Science Foundation of China (No. 81272844).

References

Bentivegna, A., Conconi, D., Panzeri, E., Sala, E., Bovo, G., Vigano, P., Brunelli, S., Bossi, M., Tredici, G., Strada, G., Dalpra, L., 2010. Biological heterogeneity of putative bladder cancer stem-like cell populations from human bladder transitional cell carcinoma samples. Cancer Sci. 101, 416–424.

Brescia, P., Richichi, C., Pelicci, G., 2012. Current strategies for identification of glioma stem cells: adequate or unsatisfactory? J. Oncol. 2012, 376894.

Cagiannos, I., Morash, C., 2009. Surveillance strategies after definitive therapy of invasive bladder cancer. Can. Urol. Assoc. J. 3, S237–S242.

Dalerba, P., Cho, R.W., Clarke, M.F., 2007. Cancer stem cells: models and concepts. Annu. Rev. Med. 58, 267–284.

Felthaus, O., Ettl, T., Gosau, M., Driemel, O., Brockhoff, G., Reck, A., Zeitler, K., Hautmann, M., Reichert, T.E., Schmalz, G., Morsczeck, C., 2011. Cancer stem cell-like cells from a single cell of oral squamous carcinoma cell lines. Biochem. Biophys. Res. Commun. 407, 28–33.

Fleetwood, A.J., Cook, A.D., Hamilton, J.A., 2005. Functions of granulocyte–macrophage colony-stimulating factor. Crit. Rev. Immunol. 25, 405–428.

Gong, C., Liao, H., Guo, F., Qin, L., Qi, J., 2012. Implication of expression of Nanog in prostate cancer cells and their stem cells. J. Huazhong Univ. Sci. Technolog. Med. Sci. 32, 242–246.

Han, M.E., Jeon, T.Y., Hwang, S.H., Lee, Y.S., Kim, H.J., Shim, H.E., Yoon, S., Baek, S.Y., Kim, B.S., Kang, C.D., Oh, S.O., 2011. Cancer spheres from gastric cancer patients provide an ideal model system for cancer stem cell research. Cell. Mol. Life Sci. 68, 3589–3605.

Hatina, J., Schulz, W.A., 2012. Stem cells in the biology of normal urothelium and urothelial carcinoma. Neoplasma 59, 728–736.

Hong, S., Li, H., Qian, J., Yang, J., Lu, Y., Yi, Q., 2012. Optimizing dendritic cell vaccine for immunotherapy in multiple myeloma: tumour lysates are more potent tumour antigens than idiotype protein to promote anti-tumour immunity. Clin. Exp. Immunol. 170, 167–177.

Hu, Z., Tan, W., Zhang, L., Liang, Z., Xu, C., Su, H., Lu, J., Gao, J., 2010. A novel immunotherapy for superficial bladder cancer by intravesical immobilization of GM–CSF. J. Cell. Mol. Med. 14, 1836–1844.

Li, L., Li, B., Shao, J., Wang, X., 2012. Chemotherapy sorting can be used to identify cancer stem cell populations. Mol. Biol. Rep. 39, 9955–9963.

Lobo, N.A., Shimono, Y., Qian, D., Clarke, M.F., 2007. The biology of cancer stem cells. Annu. Rev. Cell Dev. Biol. 23, 675–699.

McDermott, S.P., Wicha, M.S., 2010. Targeting breast cancer stem cells. Mol. Oncol. 4, 404–419.

Okamoto, A., Chikamatsu, K., Sakakura, K., Hatsushika, K., Takahashi, G., Masuyama, K., 2009. Expansion and characterization of cancer stem-like cells in squamous cell carcinoma of the head and neck. Oral Oncol. 45, 633–639.

Ou, J., Deng, J., Wei, X., Xie, G., Zhou, R., Yu, L., Liang, H., 2013. Fibronectin extra domain A (EDA) sustains CD133(+)/CD44(+) subpopulation of colorectal cancer cells. Stem Cell Res. 11, 820–833.

Pellegatta, S., Poliani, P.L., Corno, D., Menghi, F., Ghielmetti, F., Suarez-Merino, B., Caldera, V., Nava, S., Ravanini, M., Facchetti, F., Bruzzone, M.G., Finocchiaro, G., 2006. Neurospheres enriched in cancer stem-like cells are highly effective in eliciting a dendritic cell-mediated immune response against malignant gliomas. Cancer Res. 66, 10247–10252.

Scopelliti, A., Cammareri, P., Catalano, V., Saladino, V., Todaro, M., Stassi, G., 2009. Therapeutic implications of cancer initiating cells. Expert. Opin. Biol. Ther. 9, 1005–1016.

She, J.J., Zhang, P.G., Wang, Z.M., Gan, W.M., Che, X.M., 2008. Identification of side population cells from bladder cancer cells by DyeCycle Violet staining. Cancer Biol. Ther. 7, 1663–1668.

Shi, X., Zhang, X., Li, J., Guo, F., Hu, Z., Jing, Y., Bai, L., Chen, S., Wan, P., Wang, F., Gao, J., Tan, W., 2013. Sequential administration of GM–CSF and IL-2 surface-modified MB49 cells

vaccines against the metastatic bladder cancer. Urol. Oncol. 31, 883–893.

Siegel, R., Naishadham, D., Jemal, A., 2013. Cancer statistics, 2013. CA Cancer J. Clin. 63, 11–30.

Sung, J.M., Cho, H.J., Yi, H., Lee, C.H., Kim, H.S., Kim, D.K., Abd, E.A., Kim, J.S., Landowski, C.P., Hediger, M.A., Shin, H.C., 2008. Characterization of a stem cell population in lung cancer A549 cells. Biochem. Biophys. Res. Commun. 371, 163–167.

Vik-Mo, E.O., Nyakas, M., Mikkelsen, B.V., Moe, M.C., Due-Tonnesen, P., Suso, E.M., Saeboe-Larssen, S., Sandberg, C., Brinchmann, J.E., Helseth, E., Rasmussen, A.M., Lote, K., Aamdal, S., Gaudernack, G., Kvalheim, G., Langmoen, I.A., 2013. Therapeutic vaccination against autologous cancer stem cells with mRNA-transfected dendritic cells in patients with glioblastoma. Cancer Immunol. Immunother. 62, 1499–1509.

Visvader, J.E., Lindeman, G.J., 2008. Cancer stem cells in solid tumours: accumulating evidence and unresolved questions. Nat. Rev. Cancer 8, 755–768.

Weng, D., Song, B., Koido, S., Calderwood, S.K., Gong, J., 2013. Immunotherapy of radioresistant mammary tumors with early metastasis using molecular chaperone vaccines combined with ionizing radiation. J. Immunol. 191, 755–763.

Xie, Y., Wang, L., Freywald, A., Qureshi, M., Chen, Y., Xiang, J., 2013. A novel T cell-based vaccine capable of stimulating long-term functional CTL memory against B16 melanoma via CD40L signaling. Cell. Mol. Immunol. 10, 72–77.

Yanamoto, S., Kawasaki, G., Yamada, S., Yoshitomi, I., Kawano, T., Yonezawa, H., Rokutanda, S., Naruse, T., Umeda, M., 2011. Isolation and characterization of cancer stem-like side population cells in human oral cancer cells. Oral Oncol. 47, 855–860.

Zhang, X., Shi, X., Li, J., Hu, Z., Guo, F., Huang, X., Zhang, Z., Sun, P., Jing, Y., Gao, J., Tan, W., 2011. Novel immunotherapy for metastatic bladder cancer using vaccine of human interleukin-2 surface-modified MB 49 cells. Urology 78, 721–722.

Zhang, X., Shi, X., Li, J., Hu, Z., Zhou, D., Gao, J., Tan, W., 2012. A novel therapeutic vaccine of mouse GM–CSF surface modified MB49 cells against metastatic bladder cancer. J. Urol. 187, 1071–1079.